

CRATERS PRODUCED BY LARGE-SCALE EXPLOSIONS

Daniel Ambrosini^a and Bibiana Luccioni^b

^a*Facultad de Ingeniería, Universidad Nacional de Cuyo. Centro Universitario - Parque Gral. San Martín - (5500) Mendoza. Fax 54 0261 4380120. dambrosini@uncu.edu.ar, <http://leonardo.uncu.edu.ar:9673/fing/posgrados/estructural>*

^b*Instituto de Estructuras Facultad de Ciencias Exactas y Tecnología, Universidad Nacional de Tucumán Av. Roca 1800, 4000 Tucumán, Argentina. TE: 54-0381-4364087 FAX: 0381 4364087 labest@herrera.unt.edu.ar, <http://herrera.unt.edu.ar/iest>*

Keywords: Craters, explosion, blast waves, soils, hydrocode.

Abstract. In case of terrorist attacks or other intentional actions using explosives, the information that can be obtained from the crater generated by the blast waves is extremely important. For example, the focus of the explosion and the mass of the explosive used in the attack can be deduced examining the location and dimensions of the crater. However, studies about craters produced by explosions on or above ground level, which would be the case when the explosive charge is situated in a vehicle, are rarely found in the open technical literature.

A numerical study related to crater produced by small to medium explosive loads located on the soil surface was presented in previous papers. In this paper, a study about the craters created by exploding charges ranging from 120 kg to 1900 kg of TNT. The charge consists of different ordnances stacked in different configurations.

The crater diameters and depths for all explosive loads tested at the Touwsrivier Training Area (South Africa) were obtained. Moreover, the effect of the boundary conditions is analyzed and discussed.

The arrangement of the explosive load has significantly importance in the final dimensions of the crater. The final crater dimension can be larger, similar or smaller than those obtained with an equivalent spherical charge.

1 INTRODUCTION

Blasting loads have come to be forefront of attention in recent years due to a number of accidental and intentional events that affected important structures all over the world, clearly indicating that this issue is important for purposes of structural design and reliability analysis. In consequence, extensive research activities in the field of blast loads have taken place in the last few decades (Ambrosini et al. 2002).

Dynamic loads due to explosions result in strain rates of the order of 10^{-1} to 10^3 s⁻¹ which imply short time dynamic behaviour of the materials involved, characterised mainly by a great overstrength and increased stiffness, in comparison with normal, static properties. In the case of soils, the response and the mechanism of crater formation are particularly complex due to the usual anisotropy and non linear nature of the material, and to the variability of mechanical properties and coexistence of the three phases: solid, liquid and gaseous. Generally, simplifying assumptions must be made in order to solve specific problems. Until now, most practical problems have been solved through empirical approaches. Years of industrial and military experience have been condensed in charts or equations (Baker et al. 1983, Smith and Hetherington 1994). These are useful tools, for example, to establish the explosive weight to yield a perforation of certain dimensions or to estimate the type and amount of explosive used in a terrorist attack, from the damage registered. Most research is related to underground explosions and only a few papers are concerned with explosions at ground level. Studies about craters produced by explosions above ground level, which would be the case when the explosive charge is situated in a vehicle, are rarely found in the open technical literature. Some reports are classified and access is limited to government agencies.

Most of the information about explosively formed craters found in the literature is based on experimental data. Numerical studies were scarce until recently.

However, with the rapid development of computer hardware over the last years, it has become possible to make detailed numerical simulations of explosive events in personal computers, significantly increasing the availability of these methods. New developments in integrated computer hydrocodes complete the tools necessary to carry out the numerical analysis successfully. Nevertheless, it is important to be aware that both these models and analysis procedures still need experimental validation.

In previous papers (Ambrosini et al. 2004, 2006, 2007 and Luccioni et al. 2006, 2007), numerical studies related to crater produced by explosive loads located on, above or below the soil surface, and the influence of the variability of the soil properties on the crater dimensions, were presented. In this paper, a study about the craters created by exploding charges ranging from 120 kg to 1900 kg of TNT. The charge consists of different ordnances stacked in different configurations. The numerical study is related with two test programmes developed by the South African Navy (SAN) and the Blast Impact and Survivability Unit (BISRU) from the University of Cape Town (Chung Kim Yuen et al. 2008)

2 THEORY AND PREVIOUS RESULTS

A crater produced by an explosive charge situated on or above the ground level is schematized in Figure 1. The crater dimensions defined by Kinney and Graham (1985) are used in this paper (Figure 1): D is the apparent crater diameter, D_r is the actual crater diameter and H_2 is the apparent depth of the crater. The depth of the crater created by an explosion ordinarily is about one quarter of the diameter of the crater, but this ratio depends on the type of soil involved. The diameter of the crater produced by an explosion also depends on the relative location of the explosive charge to the ground level. Thus, explosions above surface level may not create any crater at all (Kinney and Graham 1985).

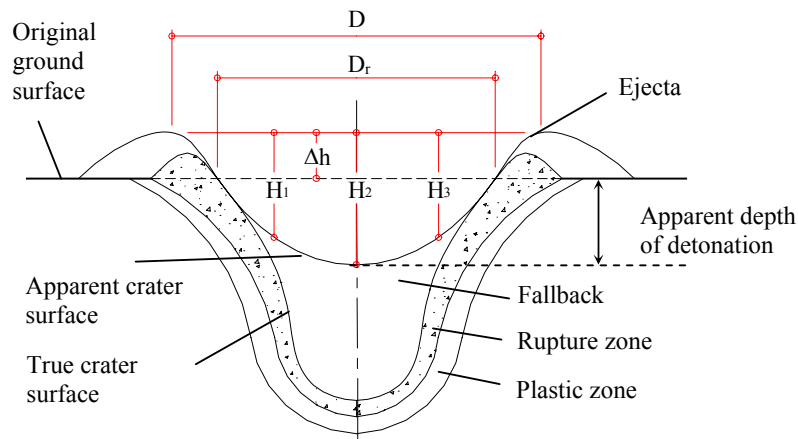


Figure 1: Definitions of the crater dimensions

Tests of crater formation are appropriate tools to study the blast phenomena, the behaviour and destructive power of different explosives and the response of soils and rocks under this type of load (Persson et al. 1994). The mechanism of crater formation is complex and it is related to the dynamic physical properties of air, soil and soil-air interface. Even very carefully performed cratering tests give deviations in the dimensions measured of the order of 10% , while differences of as much as 30% to 40% are common (Bull et al. 1998)

A cavity is always formed when a confined explosion is produced in a mass of soil. If the explosion is close to the surface, a crater is formed and a complex interaction between gravity effects, soil strength and transient load conditions takes place. The most important variables in defining the crater shape and size are the mass W of the explosive and the depth of the detonation beneath the air/soil interface d . When $d < 0$, the explosive is detonated over the air/soil interface, $d = 0$ when the detonation occurs in the air/soil interface and $d > 0$ when the explosive is detonated beneath the soil surface. For $d > 0$, the crater mechanism is altered by gravitational effects. When the depth of the detonation increases, larger amounts of subsoil must be expelled by the explosion. Thus, the crater radius and the depth of the crater increase when d increases, until a certain limit value, from which they rapidly decrease (Bull et al. 1998).

Studies concerned with the characteristics of craters caused by explosions usually resort to dimensional analysis and statistics. The scaling law establishes that any linear dimension "L" of the crater can be expressed as a constant multiplied by W^α divided by the distance of the charge from the ground, where W represents the equivalent TNT mass of explosive and α is a coefficient that is dependent on whether the gravitational effects can be neglected or not. When the gravitational effects can be neglected the cubic root law is applicable ($\alpha = 0.33$)

and in the other cases the functional dependence can be quite complex.

Baker et al. 1983 present a dimensional study to model the crater formation phenomenon in the case of underground explosions. Six parameters are chosen to define the problem: the explosive mass W , the depth of the explosive charge d , the apparent crater radius R , the soil density ρ , and two strength parameters to define the soil properties: one with the dimensions of stress σ , related to soil strength, and the other with the dimensions of a force divided by a cubic length (Nm^{-3}) K , that takes into account gravitational effects.

After a dimensional analysis and many empirical observations, the following functional relation may be obtained (Baker et al. 1983).

$$\frac{R}{d} = f \left(\frac{W^{7/24}}{\sigma^{1/6} K^{1/8} d} \right) \quad (1)$$

If $\frac{R}{d}$ (scaled radius of the crater) is plotted as a function of $W^{7/24}/d$ (Baker et al.⁷), it can be seen that this relation is close to experimental results and can be approximately simplified by two straight lines, one with a moderate slope for $W^{7/24}/d > 0.3$ and one steeper for $W^{7/24}/d < 0.3$. For $W^{7/24}/d < 0.3$, the scaled radius of the crater is sensitive to small changes in the independent parameter and, due to this fact, the independent parameter or the scaled radius may exhibit great variability. Experimental conditions are better controlled for $W^{7/24}/d > 0.3$.

The preceding paragraphs refer to underground explosions. There is less information about explosions at ground level. Statistical studies of about 200 accidental above-ground explosions of relative large magnitude are presented by Kinney and Graham (1985). The results exhibit a variation coefficient in the crater diameter of about 30%. From these results, the following empirical equation for the crater diameter was proposed.

$$D [m] = 0.8W[Kg]^{1/3} \quad (2)$$

In connection with the morphological and structural types of the craters, Melosh (1989) determine four different basic types: (a) bowl-shaped, (b) flat-floored with central uplift, (c) flat floored with a peak ring and (d) flat floored with >2 asymmetric rings (multiring basins). One of the factors that determine the shape is the height of burst. On the other hand, numerical and independent research results presented by Iturrioz et al. (2001) preliminary confirm the formation of the same shapes of craters. Additionally, there are important contributions in the literature related to cratering studies, but many of them are about predicting *rock* damage, ex. Yang et al. (1996), Liu and Katsabanis (1997) and Wu et al. (2004) and others are related with *buried* explosions, ex. Wang and Lu (2003) and Zhou et al. (2003).

On the other hand, Ambrosini and Luccioni (2006) proposed the following equations for the prediction of crater dimensions for spherical explosive charges situated on the ground (case a) and with the energy release center at ground level (case b) respectively. These equations represent the linear approximation of numerical result by minimum least-fit squares. The variation of $\pm 5\%$ accounts for the differences between soil properties that could be found in different sites.

Case (a)  $D [m] = 0.51W [Kg]^{1/3} \pm 5\%$ (3)

Case (b)  $D [m] = 0.65W [Kg]^{1/3} \pm 5\%$ (4)

In a previous paper, Ambrosini et al. (1998) presented the results of a series of tests performed with different amounts of explosive at short distances above and below ground level, as well as on the soil surface. These results were used in this paper to calibrate the soil parameters of the numerical model as well as to validate the analysis procedure. The description of the tests as well as the numerical-experimental comparison and the model calibration was presented by Ambrosini and Luccioni (2007).

3 CASE STUDY

The numerical study is related with two test programmes developed by the South African Navy (SAN) and the Blast Impact and Survivability Unit (BISRU) from the University of Cape Town, one at Eikenboshhoek Range, Touwsrivier Training Area in November 2004 and the other at the Vastrap Weapons Range in November 2006 (Chung Kim Yuen et al. 2008).

In this paper, only the case from Touwsrivier Training Area will be considered. These tests were conducted on the Eikenboshhoek Range at the Touwsrivier Training Area for the South African Defence Divisions over three days. This test range is located approximately 200km north of Cape Town. The general terrain of the test area is a large open, fairly flat, gravel space surrounded by shrubs and bushes. Eight blast tests will be considered, with characteristics listed in Table 1.

The blasts resulted from the detonation of ordnance such as – Projectile AS MK 10 (mass nominally 100kg); Warhead KC5 (mass nominally 200kg) and Warhead KC9 (mass nominally 300kg). The KC5/KC9 warheads were filled with Amatol explosives, which consisted of 50%TNT and 50% Ammonium nitrate. The AS MK 10 Projectile was filled with Minol explosives, which had a composition of 40%TNT, 40% Ammonium nitrate and 20% aluminium (Chung Kim Yuen et al. 2008).

Each blast test consists of an assembly of ordnance, comprising items shown in Figure 2, as required to configure the predetermined mass. PE4 was used as booster to initiate the blast.

Blast No.	Charge mass (kg)	Ordnance	TNT equivalent W (kg)
1	100	AS MK 10 (x1)	120
2	200	KC5 (x1)	190
3	400	KC5 (x2)	380
4	700	KC5 (x2) KC9 (x1)	665
5	1000	KC5 (x2) KC9 (x2)	950
6	1300	KC9 (x4) AS MK 10 (x1)	1260
7	2000	KC9 (x6) KC5 (x1)	1900
8	200	AS MK 10 (x1)	240

Table 1: Test data considered in the numerical analysis.

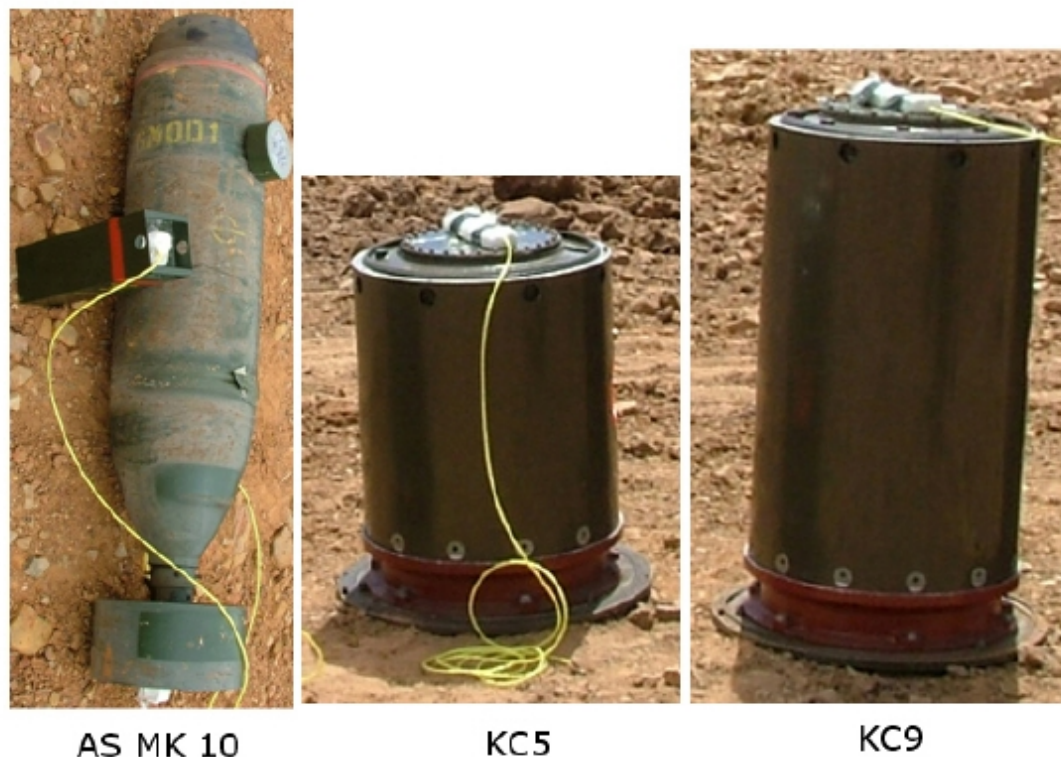


Figure 2: Ordnance used to configure the blast assembly (Chung Kim Yuen et al. 2008).

Unfortunately, at present, are not available the experimental results from the craters generated by the explosions. Then, in this paper, only the numerical results are presented. In future papers a numerical-experimental comparison about the Touwsrivier test will be presented.

4 NUMERICAL MODEL

4.1 Introduction and numerical tool

Computer codes normally referred as “hydrocodes” encompass several different numerical techniques in order to solve a wide variety of non-linear problems in solid, fluid and gas dynamics. The phenomena to be studied with such a program can be characterized as highly time dependent with both geometric non-linearities (e.g. large strains and deformations) and material non-linearities (e.g. plasticity, failure, strain-hardening and softening, multiphase equations of state). Different numerical tools are used in some papers in order to solve similar problems of crater determination. For example ABAQUS (Yang et al. 1996), AUTODYN (Wu et al. 2004, Wang and Lu 2003), SALE2D (Baratoux and Melosh 2003, Nolan et al. 2001) and CTH (Pierazzo and Melosh 1999).

In this paper, the software AUTODYN-3D (2007), which is a “hydrocode” that uses finite difference, finite volume, and finite element techniques to solve a wide variety of non-linear problems in solid, fluid and gas dynamics, is used. The phenomena to be studied with such a program can be characterized as highly time dependent with both geometric non-linearities (e.g. large strains and deformations) and material non-linearities (e.g. plasticity, failure, strain-hardening and softening, multiphase equations of state).

The various numerical processors available in AUTODYN generally use a coupled finite

difference/finite volume approach similar to that described by Cowler and Hancock (1979). This scheme allows alternative numerical processors to be selectively used to model different components/regimes of a problem. Individual structured meshes operated on by these different numerical processors can be coupled together in space and time to efficiently compute structural, fluid, or gas dynamics problems including coupled problems (e.g. fluid-structure, gas-structure, structure-structure, etc.).

AUTODYN includes the following numerical processors: Lagrange, Euler, ALE, Shell, Euler-Godunov, Euler-FCT and SPH. All the above processors use explicit time integration. The first-order Euler approach scheme is based on the method developed by Hancock (1976).

While finite element codes are usually based on the equilibrium condition, the hydrocode utilizes the differential equations governing unsteady material dynamic motion: the local conservation of mass, momentum and energy. In order to obtain a complete solution, in addition to appropriate initial and boundary conditions, it is necessary to define a further relation between the flow variables. This can be found from a material model, which relates stress to deformation and internal energy (or temperature). In most cases, the stress tensor may be separated into a uniform hydrostatic pressure (all three normal stresses equal) and a stress deviatoric tensor associated with the resistance of the material to shear distortion.

The relation between the hydrostatic pressure, the local density (or specific volume) and local specific energy (or temperature) is known as an equation of state. Since solids are able to withstand a certain amount of tensile stress, it is necessary to consider extending the equations of state into limited regions of negative values of the pressure (tension). However, since the analytic forms derived for ranges of positive pressure it may not be valid for extrapolation into the negative regions special attention should be paid in using some forms of equation of state. The *hydrodynamic tensile limit*, sometimes referred to as p_{min} , is the minimum pressure to which the material can sustain continuous expansion. If the material pressure drops below this limit in a cell it is assumed that the material will fracture, or in some way lose its uniform and continuous ability to sustain a tensile pressure. This would then form the lower limit of the analytic equation of state. Regardless the definition of a value of p_{min} it may be necessary to provide a different analytic form for negative pressure values from that used for positive values (but taking care to ensure continuity of function and derivatives at $p = 0$).

While there are many problems that can be calculated using a hydrodynamic equation of state, there are many applications where material strength effects (i.e. its resistance to shearing forces) cannot be ignored and indeed may even dominate. If the material is solid and has finite shear strength then, in addition to the calculation of the hydrostatic pressure, it is necessary to define relations between shear stress and strain. The methodology followed in this paper is that first one formulated by Wilkins (1964) to extend conventional numerical hydrodynamic codes to include the effects of material strength and resistance to shear distortion.

A relation to define the transition between elastic and plastic strain, both in compression and release, and a relation to define the onset of fracture, are also required. The yield criterion governing the transition from elastic to plastic behaviour may involve only constant yield strength, or this strength may itself be a function of the degree of strain (work hardening), the rate of strain and/or the temperature of the material (energy dependency).

Real materials are not able to withstand tensile stresses that exceed the material local tensile strength. The computation of the dynamic motion of materials assuming that they always remain continuous, even if the predicted local stresses reach very large negative values, will lead to unphysical solutions. For this reason the model has to be constructed to

recognize when tensile limits are reached, to modify the computation to deal with this and to describe the properties of the material after this formulation has been applied.

4.2 Numerical meshes

In this paper, an Euler Godunov processor is used to model the air and the explosive charge as well as for the soil. Due to the geometrical configuration of the differentes ordnances listed in Table 1, only for the blast2 case the use of symmetry conditions allows using a two-dimensional (2D) mesh considering axial symmetry. For the remaining ordnances, a 3D model was used with planar symmetry in some cases. The numerical models for the different cases listed in Table 1 are presented in Figures 3 to 9. In all cases, in order to facilitate the visualization, the air is not showed. The detonation point is represented by a red point.

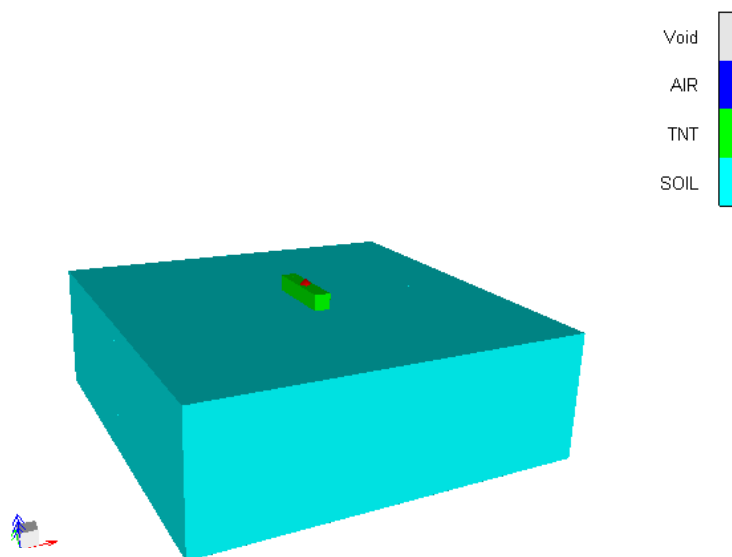


Figure 3: Numerical model for blast1. 120 kg of TNT. Planar symmetry about xz and yz planes.
Mesh: $x = 3.00\text{m}$ (6.00m); $y = 3.00\text{m}$ (6.00m); $z = 2.00\text{m}$ (soil) 1.00m (air)

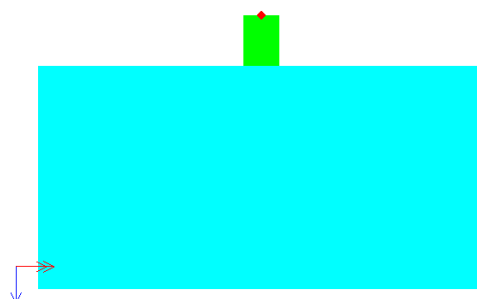


Figure 4: Numerical model for blast2. 190 kg of TNT. Axial symmetry. 2D model.
Mesh: $6\text{m} \times 3\text{m}$ mesh representing a 6m -diameter cylinder

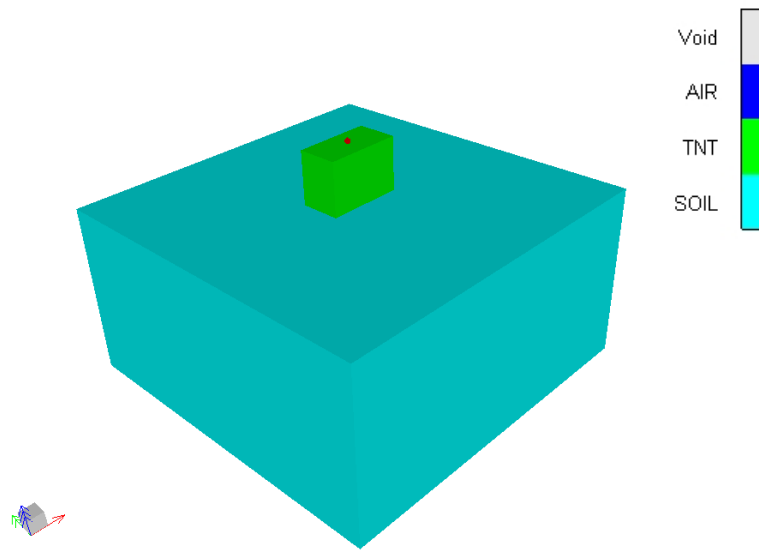
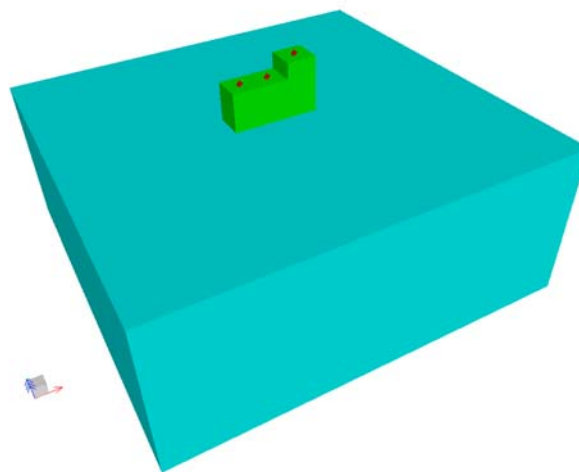


Figure 5: Numerical model for blast3. 380 kg of TNT.
Mesh: $x = 4.00\text{m}$; $y = 4.00\text{m}$; $z = 2.00\text{m}$ (soil) 2.00m (air)

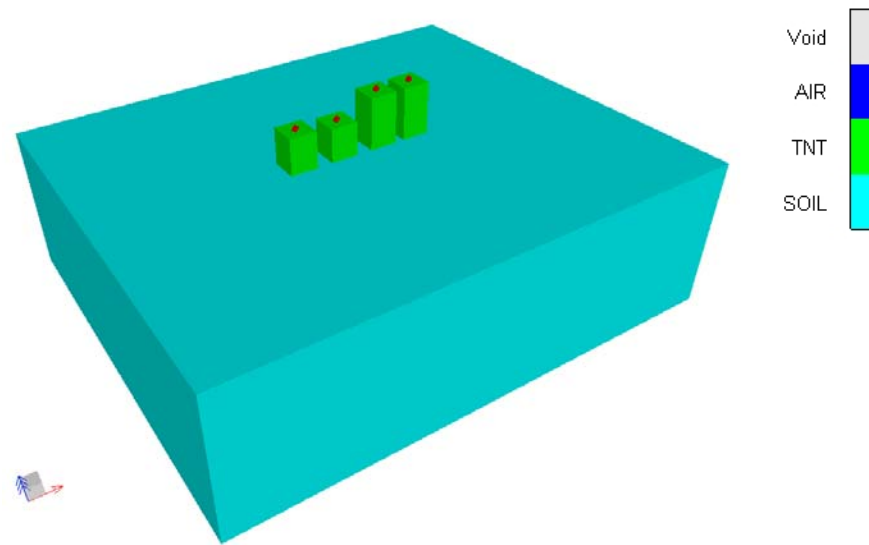


(a)



(b)

Figure 6: a) Numerical model for blast4. 665 kg of TNT. Planar symmetry about xz plane.
Mesh: $x = 6.30\text{m}$; $y = 3.00\text{m}$ (6.00m); $z = 2.50\text{m}$ (soil) 2.50m (air)
b) Photograph of the arrangement of the test from Chung Kim Yuen et al. (2008)



(a)



(b)

Figure 6: a) Numerical model for blast5 (half). 950 kg of TNT. Planar symmetry about xz plane.
 Mesh: $x = 8.45\text{m}$; $y = 3.50\text{m}$ (7.00m); $z = 2.50\text{m}$ (soil) 2.50m (air)
 b) Photograph of the arrangement of the test from Chung Kim Yuen et al. (2008)

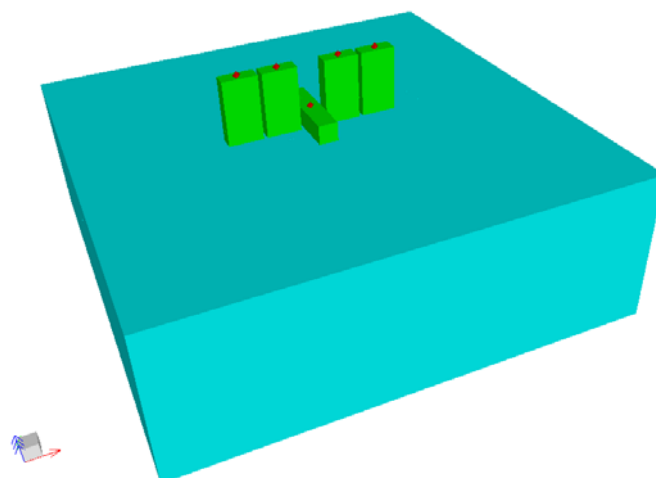
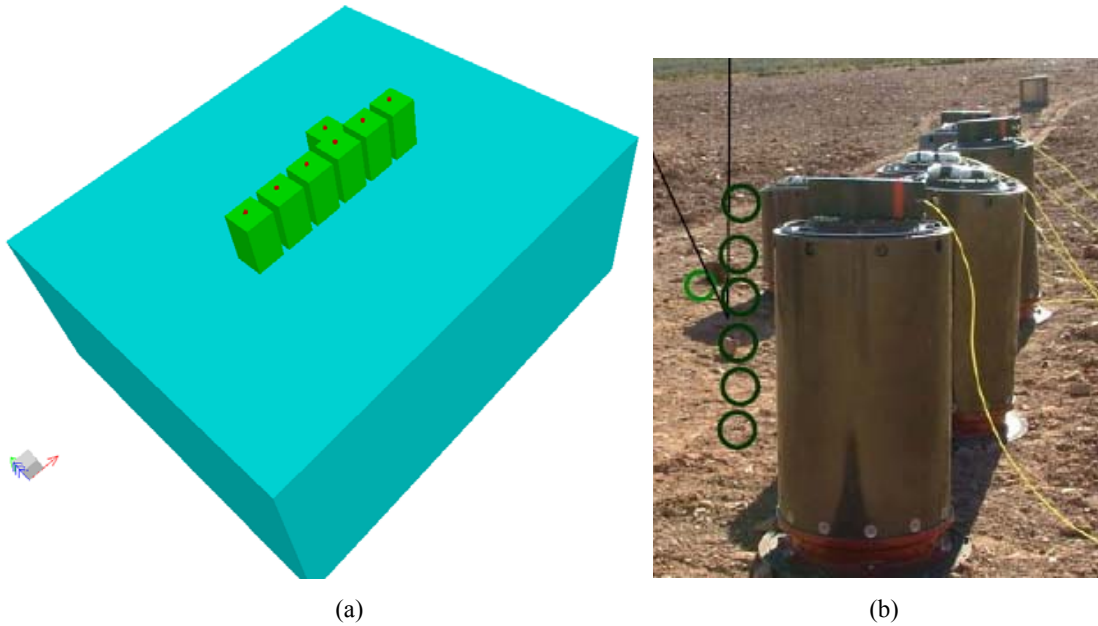
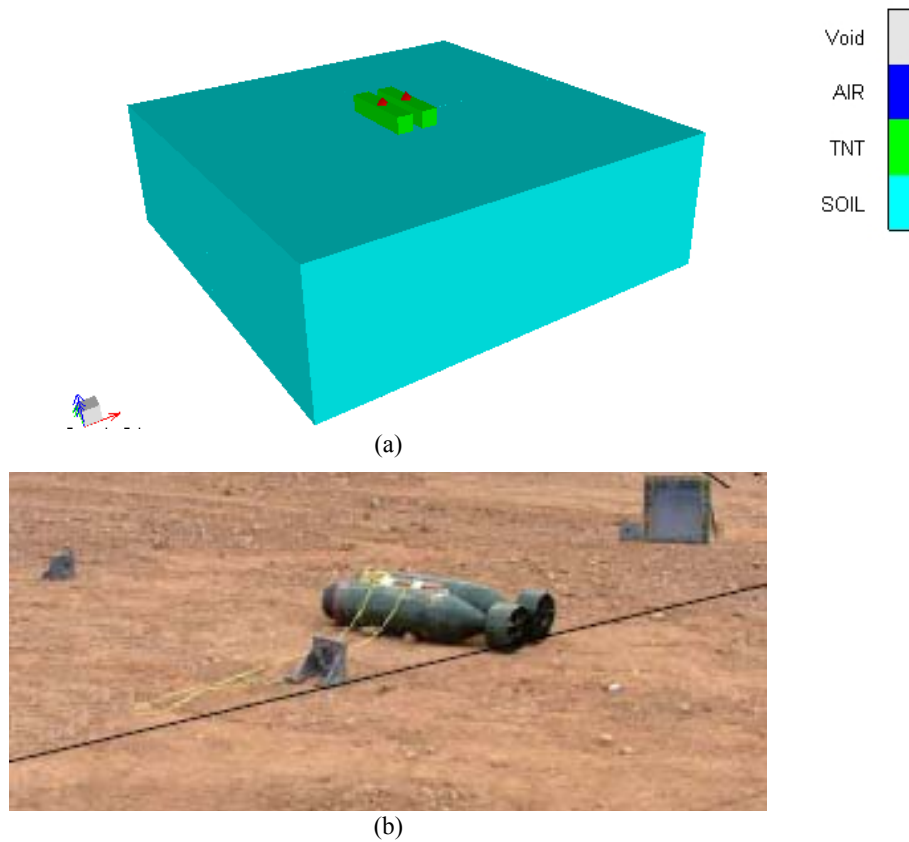


Figure 7: a) Numerical model for blast6. 1260 kg of TNT. Planar symmetry about xz and yz planes.
 Mesh: $x = 3.00\text{m}$ (6.00m); $y = 3.00\text{m}$ (6.00m); $z = 2.00\text{m}$ (soil) 1.50m (air)



(a) Numerical model for blast7. 1900 kg of TNT. Full 3D.
 Mesh: $x = 7.20\text{m}$; $y = 5.90\text{m}$; $z = 3.00\text{m}$ (soil) 3.00m (air)
 (b) Photograph of the arrangement of the test from Chung Kim Yuen et al. (2008)



(a) Numerical model for blast8. 240 kg of TNT. Planar symmetry about xz plane.
 Mesh: $x = 6.30\text{m}$; $y = 3.00\text{m}$ (6.00m); $z = 2.50\text{m}$ (soil) 2.50m (air)
 (b) Photograph of the arrangement of the test from Chung Kim Yuen et al. (2008)

4.3 Materials models

a) *Air*: The ideal gas equation of state was used for the air. This is one of the simplest forms of equation of state for gases. In an ideal gas, the internal energy is a function of the temperature alone and if the gas is polytropic the internal energy is simply proportional to temperature. It follows that the equation of state for a gas, which has uniform initial conditions, may be written as,

$$p = (\gamma - 1)\rho e \quad (5)$$

in which p is the hydrostatic pressure, ρ is the density and e is the specific internal energy. γ is the adiabatic exponent, it is a constant (equal to $1 + R/c_v$) where constant R may be taken to be the universal gas constant R_0 divided by the effective molecular weight of the particular gas and c_v is the specific heat at constant volume.

b) *TNT*: High explosives are chemical substances which, when subject to suitable stimuli, react chemically very rapidly (in order of microseconds) releasing energy. In the hydrodynamic theory of detonation, this very rapid time interval is shrunk to zero and a detonation wave is assumed to be a discontinuity which propagates through the unreacted material instantaneously liberating energy and transforming the explosive into detonating products. The normal Rankine-Hugoniot relations, expressing the conservation of mass, momentum and energy across the discontinuity may be used to relate the hydrodynamic variables across the reaction zone. The only difference between the Rankine-Hugoniot equations for a shock wave in a chemically inert material and those for a detonation wave is the inclusion of a chemical energy term in the energy conservation equation.

Since the 1939-45 war, when there was naturally extensive study of the behaviour of high explosives, there has been a continuous attempt to understand the detonation process and the performance of the detonation products, leading to considerable improvements in the equation of state of the products. The most comprehensive form of equation of state developed over this period, the "Jones - Wilkins - Lee" (JWL) equation of state, is used in this paper.

$$p = C_1 \left(1 - \frac{\omega}{r_1 v}\right) e^{-r_1 v} + C_2 \left(1 - \frac{\omega}{r_2 v}\right) e^{-r_2 v} + \frac{\omega e}{v} \quad (6)$$

Where $v = 1/\rho$ is the specific volume, C_1 , r_1 , C_2 , r_2 and ω (adiabatic constant) are constants and their values have been determined from dynamic experiments and are available in the literature for many common explosives.

It can be shown that at large expansion ratios the first and second terms on the right hand side of Equation (4) become negligible and hence the behaviour of the explosive tends towards that of an ideal gas. Therefore, at large expansion ratios, where the explosive has expanded by a factor of approximately 10 from its original volume, it is valid to switch the equation of state for a high explosive from JWL to ideal gas. In such a case the adiabatic exponent for the ideal gas, γ , is related to the adiabatic constant of the explosive, ω , by the relation $\gamma = \omega + 1$. The reference density for the explosive can then be modified and the material compression will be reset. Potential numerical difficulties are therefore avoided.

An explosion may be initiated by various methods. However, whether an explosive is dropped, thermally irradiated or shocked, either mechanically or from a shock from an initiator (of more sensitive explosive), initiation of an explosive always goes through a stage in which a shock wave is an important feature. Lee-Tarver equation of state (Lee and Tarver 1980) was used to model both the detonation and expansion of TNT in conjunction with JWL EOS to model the unreacted explosive.

c) *Soil*: A shock equation of state combined with an elastoplastic strength model based on Mohr Coulomb criterion and a hydro tensile limit were used for the soil.

A Mie-Gruneisen form of equation of state based on the shock Hugoniot was used. The Rankine-Hugoniot equations for the shock jump conditions can be regarded as defining a relation between any pair of the variables ρ , p , e , u_p (material velocity behind the shock) and U (shock velocity). In many dynamic experiments it has been found that for most solids and many liquids over a wide range of pressure there is an empirical linear relationship between u_p and U .

$$U = c_0 + s u_p \quad (7)$$

in which c_0 is the initial sound speed and s a dimensionless parameter.

This is the case even up to shock velocities around twice the initial sound speed c_0 and shock pressures of order 100 GPa. In this case the equation of state is:

$$p = p_H + \Gamma \rho (e - e_H) \text{ with } p_H = \frac{\rho_0 c_0^2 \mu (1 + \mu)}{[1 - (s-1)\mu]^2}; \quad e_H = \frac{1}{2} \frac{p_H}{\rho_0} \frac{\mu}{1 + \mu}; \quad \mu = \frac{\rho}{\rho_0} - 1 \quad (8)$$

where p is the hydrostatic pressure, ρ_0 is the initial density, e is the specific internal energy and Γ is the Gruneisen Gamma parameter and it is assumed that $\Gamma \rho = \Gamma_0 \rho_0 = \text{const}$

An elastoplastic model with Mohr Coulomb yield criterion was used for the strength effects. This model is an attempt to reproduce the behaviour of dry soil where the cohesion and compaction result in an increasing resistance to shear up to a limiting value of yield strength as the loading increases. This is modelled by a piecewise linear variation of yield stress with pressure. In tension (negative values of p) soils have little tensile strength and this is modelled by dropping the curve for $Y(p)$ rapidly to zero as p goes negative to give a realistic value for the limiting tensile strength.

A non associated flow rule (Prandtl-Reuss type) that avoids the problem of shear induced dilatancy in soils was used. A constant HTL was specified as failure criterion.

All the material properties used for the models are presented in Ambrosini et al. (2003).

4.4 Boundary transmit

In order to fulfil the radiation condition, a transmitting boundary was defined for air as well as soil subgrids external limits. The Transmit Boundary condition allows a stress wave to continue "through" the physical boundary of the subgrid without reflection. The size of the numerical mesh can be reduced by use of this boundary condition. The transmit boundary is only active for flow out of a grid. The transmit boundary is calculated as follows:

Let the normal velocity at the boundary be U_n , where U_n is positive for outflow. Then the boundary pressure (P) is computed as follows:

For $U_n > 0$:

$$P = P_{ref} + (U_n - U_{ref})I \quad (9)$$

For $U_n < 0$:

$$P = P_{ref} \quad (10)$$

in which P_{ref} and U_{ref} are the pressure and velocity of reference respectively (material model properties) and I is the material impedance (density*soundspeed). If the impedance at the boundary is undefined, it is taken from values in adjacent cells.

5 RESULTS AND DISCUSSION

The process of crater formation and crater dimension for the explosive charges listed in Table 1 was analyzed with the procedure described.

5.1 Final crater

The final crater obtained in the analysis is presented in Figures 10 to 17. In all cases, in order to facilitate the visualization, as the air as the TNT, are not showed.

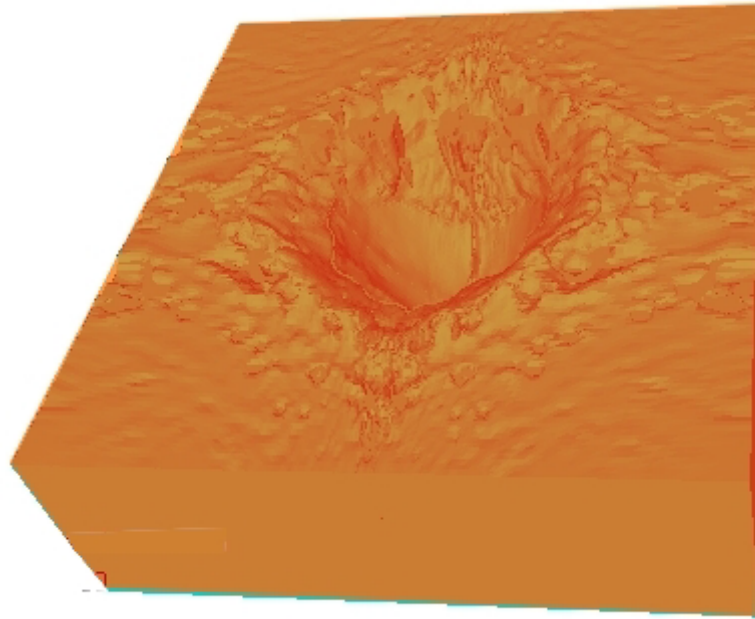


Figure 10: Final crater. Blast1. 120 kg TNT

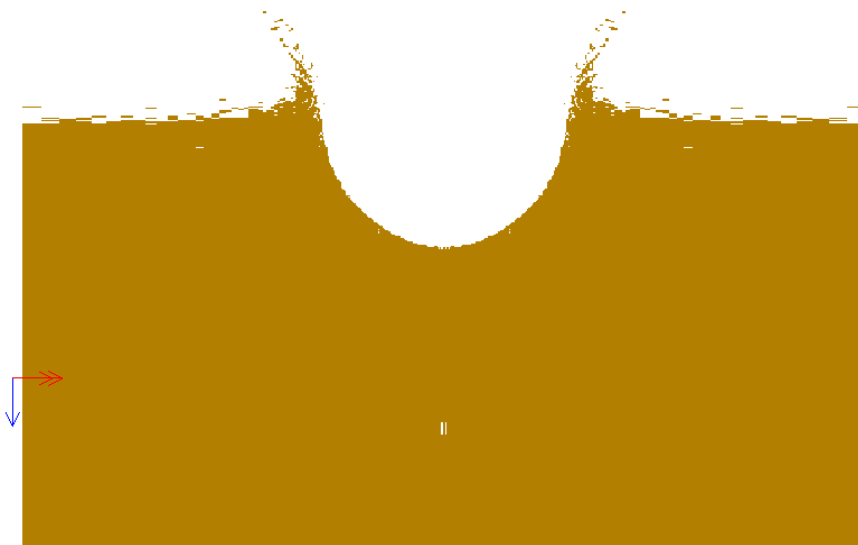


Figure 11: Final crater. Blast2. 190 kg TNT

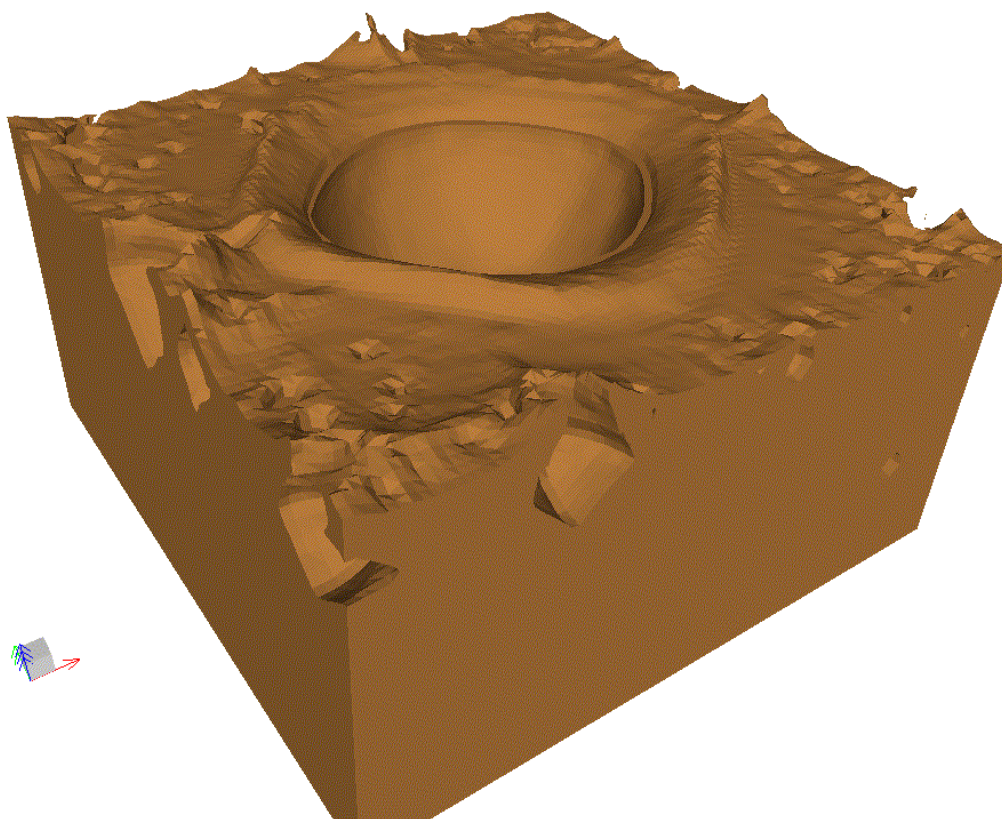


Figure 12: Final crater. Blast3. 3800 kg TNT

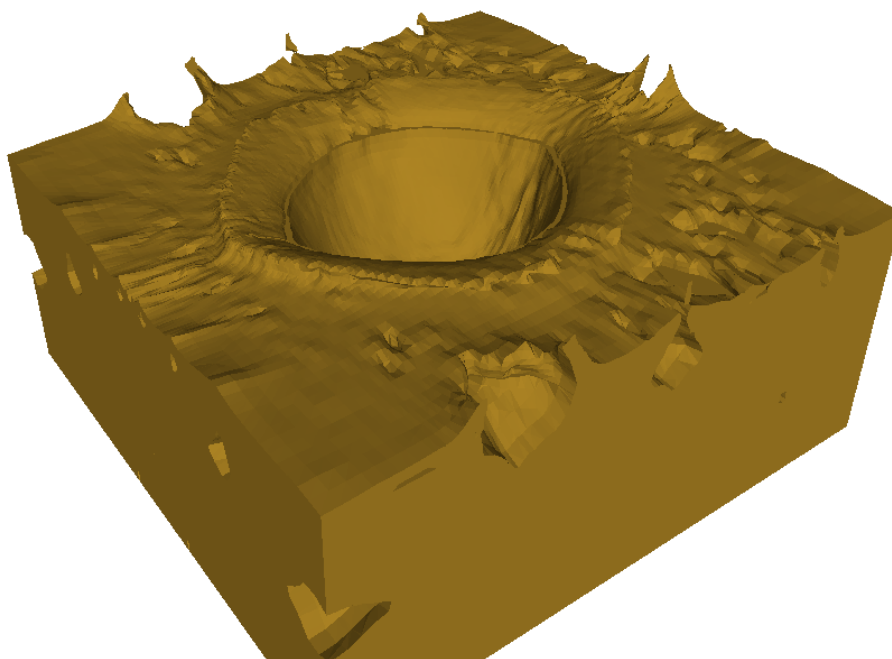


Figure 13: Final crater. Blast4. 665 kg TNT

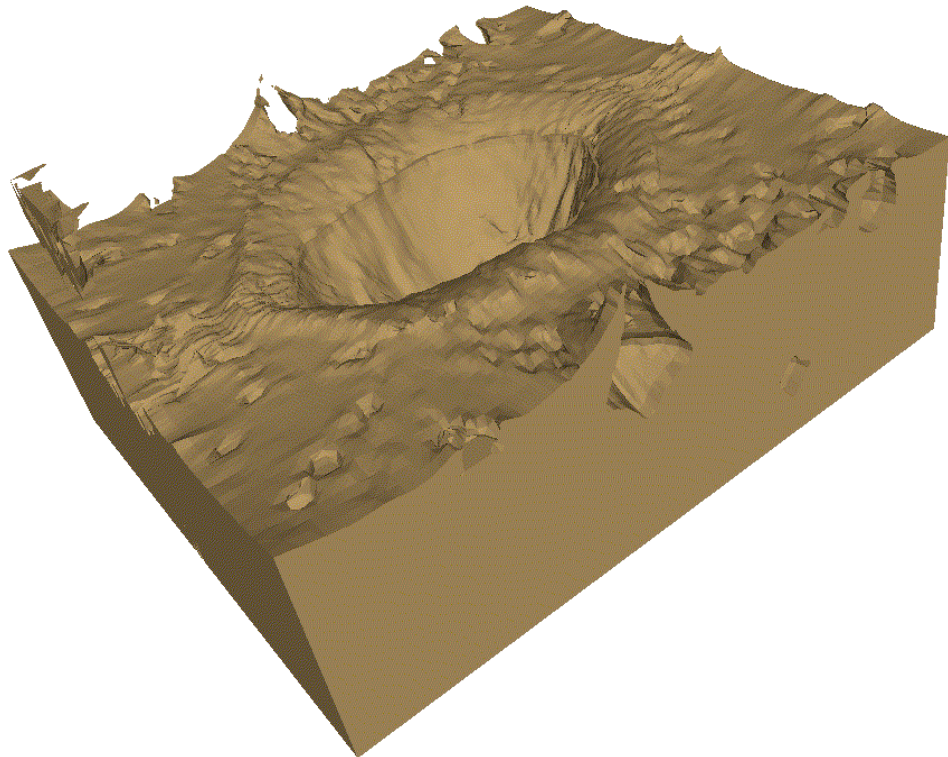


Figure 14: Final crater. Blast5. 950 kg TNT

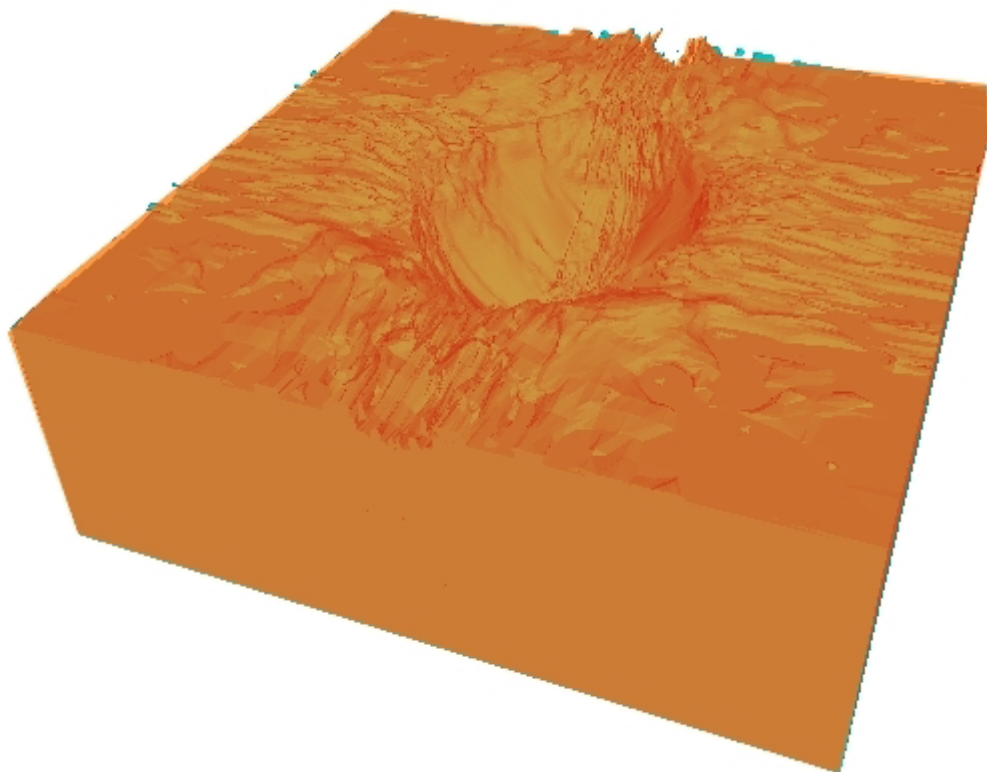


Figure 15: Final crater. Blast6. 1260 kg TNT

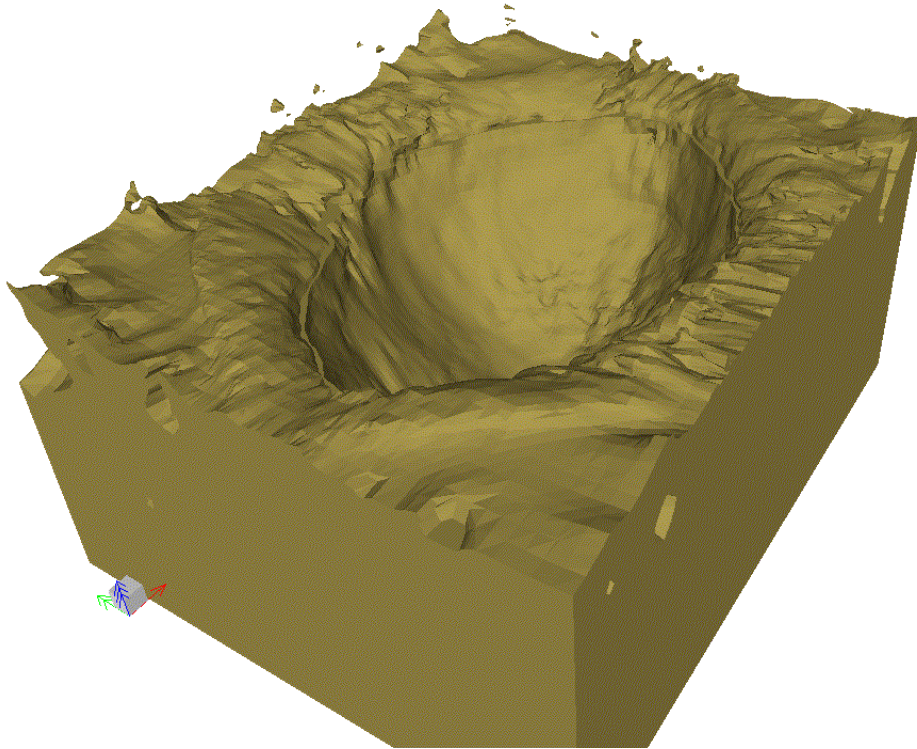


Figure 16: Final crater. Blast7. 1900 kg TNT

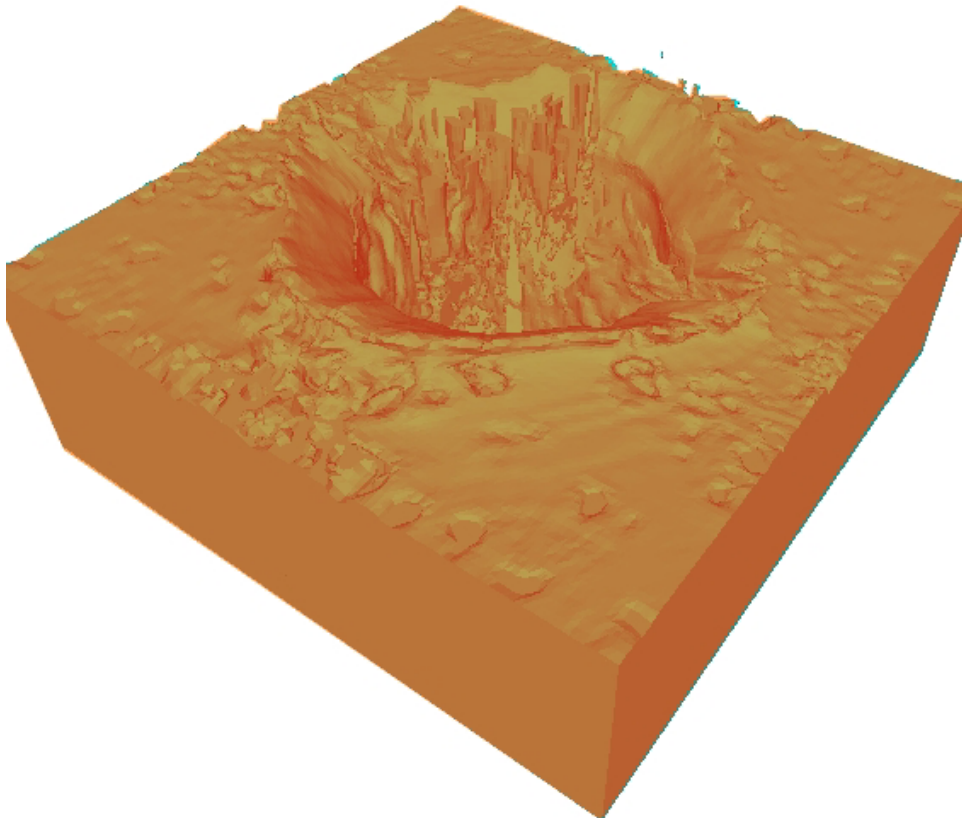


Figure 17: Final crater. Blas8. 240 kg TNT

It is clear from some pictures (e.g. Figures 12 to 14) that the transmitting boundary allows some reflection of the stress wave. Then, it would be necessary to use a larger mesh in some cases. However, after some tests for various cases, the obtained results demonstrates that this reflection do not significantly affect the final dimensions of the crater.

5.2 Numerical results

The crater dimensions for all cases listed in Table 1 are presented in Table 2. For all cases, except blast2, due to the particular arrangement of the explosive loads, the final crater is not symmetrical. Then, the crater dimensions about x and y axes are presented in Table 2. In the case blast5, H is not uniform and then, two representative values are presented. In the case blast 7, D_y is not uniform and then, three representative values are presented.

It must be pointed out that, in most cases it is difficult to "measure" the final crater. As an example, in Figure 18, two ways to measure the crater are presented. Then, in some cases, the two measures are indicated. This drives to some uncertainties in the final measure of the crater, which are common in this type of the analysis. The comparison with the experimental results, which will be presented in subsequent papers, lead to a better adjust of the numerical models.

Blast No.	Charge mass W (kg TNT)	D_x m	D_y m	H m
1	120	3.36 2.51 ^a	3.80	1.40
2	190	2.02 2.93 ^a		0.89
3	380	3.00 3.69 ^a	2.70	1.00
4	665	4.26 4.49 ^b 4.45 ^a	3.92	2.10
5	950	5.08 5.38 ^b 5.01 ^a	3.65	1.40 and 1.60
6	1260	4.51 5.51 ^a	3.54	1.40
7	1900	5.72 5.84 ^b 6.32 ^a	3.57 4.42 In the middle: 3.91m	2.12
8	240	3.96 3.17 ^a	4.70	1.75

^a obtained with equation (3) for spherical charges.

^b measure 2 (see Figure 18)

Table 2: Numerical results obtained. Dimensions of the crater.

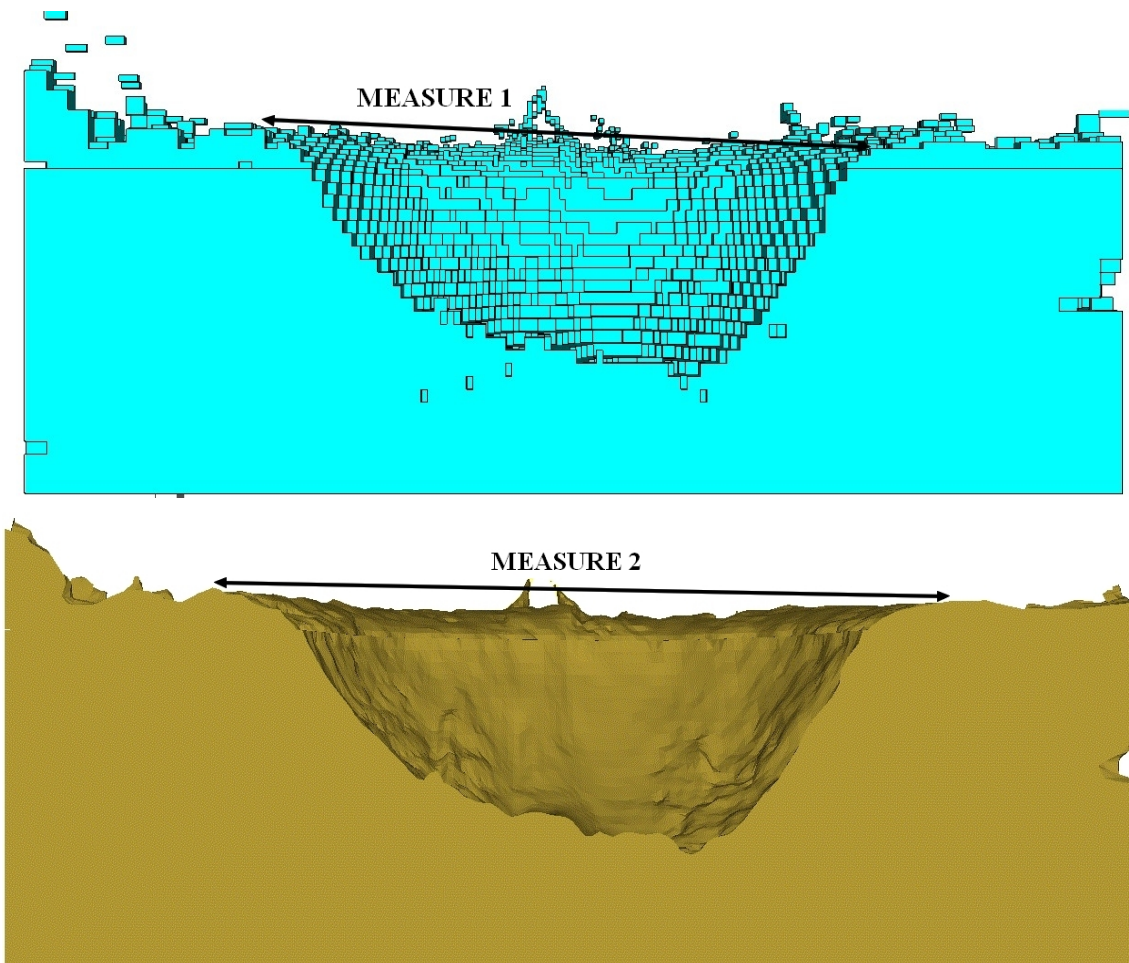


Figure 18: Two ways to measure the final crater

It may be observed that the different arrangements affect significantly the final dimensions of the crater. In some cases, blast1 and blast8 (AS MK 10 Projectile in horizontal position) the crater obtained is larger than those obtained with an equivalent spherical charge. In other cases, blast2 and blast3 (Warhead KC5 in vertical position) the crater obtained is smaller than those obtained with an equivalent spherical charge. In the remaining cases, the mean dimension of the crater is comparable with those obtained with an equivalent spherical charge.

It must be pointed out that, as it was demonstrated by Ambrosini et al. (2004), the elastic properties of the soil do not affect significantly the diameter of the crater. However, a variation of $\pm 5\%$ could be obtained in particular cases.

6 CONCLUSIONS

A numerical study about the craters created by exploding charges ranging from 120 kg to 1900 kg of TNT is presented in this paper. The charge consists of different ordnances stacked in different configurations and are related with two test programmes developed by the South African Navy (SAN) and the Blast Impact and Survivability Unit (BISRU) from the University of Cape Town.

The crater diameters and depths for all explosive loads tested at the Touwsrivier Training Area (South Africa) were obtained. Based on the obtained results, the following conclusions must be drawn:

- The transmitting boundary of the numerical tool allows some reflection of the stress wave and need to be optimized or, alternatively, a larger numerical mesh should be used. However, the obtained results demonstrates that this reflection do not significantly affect the final dimensions of the crater.
- The arrangement of the explosive load has significantly importance in the final dimensions of the crater. The final crater dimension can be larger, similar or smaller than those obtained with an equivalent spherical charge.
- Some uncertainties appear in the measurement of the numerical crater because the top of the soil in the ejecta is not clearly defined in some cases.

In future papers, the comparison with the experimental results will be presented.

ACKNOWLEDGEMENTS

The authors wish to thank to Prof. Gerald Nurick (BISRU, University of Cape Town) for facilitating the data of the blast loading tests.

Moreover, the financial support of the CONICET (Argentina), SECYT (National University of Cuyo) and CIUNT (National University of Tucumán) is gratefully acknowledged.

REFERENCES

- Ambrosini D., Luccioni B.M., Danesi R.F., Riera J.D. and Rocha M.M. Size of Craters Produced by Explosive Charges on or Above the Ground Surface. *Shock Waves*, 12(1), 69-78, 2002.
- Ambrosini D., B. Luccioni and R. Danesi. Craters produced by explosions on the soil surface. *Computational Mechanics*, XXII:678-692, 2003.
- Ambrosini D., B. Luccioni and R. Danesi. Influence of the soil properties on craters produced by explosions on the soil surface. *Computational Mechanics*, XXIII, 571-590, 2004.
- Ambrosini D. and B. Luccioni. Craters produced by explosions on the soil surface. *Journal of Applied Mechanics, ASME*, 73(6), 890-900. 2006
- Ambrosini, D. and B. Luccioni. Craters produced by explosions above the soil surface. *Computational Mechanics*, XXVI, 2253-2266, 2007.
- AUTODYN. *Interactive Non-Linear Dynamic Analysis Software*, Version 11.0, User's Manual. Century Dynamics Inc., 2007
- Baker W.E., Cox P.A., Westine P.S., Kulesz J.J., Strehlow R.A., *Explosion hazards and evaluation*. Elsevier, Amsterdam. 1983.
- Baratoux D, Melosh HJ. The formation of shatter cones by shock wave interference during impacting. *Earth and Planetary Science Letters*, 216, 43-54. 2003.
- Bull JW, Woodford CH, Camouflets and their effects on runway supports. *Computer and Structures*, 69/6, 695-706, 1998.

- Chung Kim Yuen S, Nurick GN, Verster W, Jacob N, Vara AR, Balden VH, Bwalya D, Govender RA, Pittermann M. Deformation of mild steel plates subjected to large-scale explosions. *International Journal of Impact Engineering*, 35(8), 684-703, 2008.
- Cowler MS, Hancock SL. Dynamic fluid-structure analysis of shells using the PISCES 2DELK computer code. *5th Int. Conf. on Structural Dynamics in Reactor Technology*, Paper B1/6, 1979.
- Gorodilov LV, Sukhotin AP, Experimental investigation of craters generated by explosions of underwater surface charges on sand. *Combustion, Explosion, and Shock Waves*, 32(3), 344-346, 1996.
- Hancock S. Finite Difference Equations for PISCES-2DELK, TCAM-76-2, *Physics International*, 1976.
- Hara A, Ohta T, Niwa M, Tanaka S, Banno T. Shear modulus and shear strength of cohesive soils. *Soils and Foundations*, 14, 1-12. 1974.
- Iturrioz I, Riera JD, Numerical Study of the Effect of Explosives on a Plane Surface, *XII Congress on Numerical Methods and their Applications, ENIEF 2001*, Arg. 2001.
- Jones GHS, Roddy DJ, Henny RW, Slater JE, Defence Research Establishment Suffield Explosion Craters and Planetary Impact Craters: Morphological and Structural Deformation Analogues, *15th International Symposium on Military Aspect of Blast and Shock*, Alberta, Canada 1997.
- Kinney G.F., Graham K.J. *Explosive shocks in air*. 2nd Edition, Springer Verlag, 1985.
- Lee, E. L., & Tarver, C. M.. Phenomenological Model of Shock Initiation in Heterogeneous Explosives. *Physics of Fluids*, 23 (12), 2362-2372 1980.
- Luccioni B. and D. Ambrosini. Craters produced by underground explosions. *Computational Mechanics*, XXV, 1603-1614, 2006.
- Luccioni B. and D. Ambrosini. Effect of buried explosions.. *Computational Mechanics*, XXVI, 2656-2673, 2007.
- Nolan MC, Asphaug E, Greenberg R, Melosh HJ. Impacts on Asteroids: Fragmentation, Regolith Transport, and Disruption. *Icarus* 153, 1-15, 2001.
- Ohsaki Y, Iwasaki R. On dynamic shear moduli and Poisson's ratios of soil deposits. *Soils and Foundations*, 13, 61-73. 1973
- Persson PA, Holmberg R., Lee J, *Rock blasting and explosives engineering*, CRC Press, USA, 540 ps 1994.
- Pierazzo E, Melosh HJ. Hydrocode modeling of Chicxulub as an oblique impact event. *Earth and Planetary Science Letters*, 165, 163-176, 1999.
- Smith PD, Hetherington JG, *Blast and Ballistic Loading of Structures*, Butterworth-Heinemann Ltd, Great Britain. 1994.
- Wang Z., Lu Y. Numerical analysis on dynamic deformation mechanism of soils under blast loading, *Soil Dynamics and Earthquake Engineering*, 23, 705-714. 2003.
- Wilkins, M. L. Calculation of Elastic-Plastic Flow, *Methods of Computational Physics*, 3, 211-263 1964.
- Wu C., Lu Y, Hao H. Numerical prediction of blast-induced stress wave from large-scale underground explosion, *International Journal for Numerical and Analytical Methods in Geomechanics*, 28, 93-109. 2004.
- Yang R, Bawden WF, Katsabanis PD. A New Constitutive Model for Blast Damage, *Int. J. Rock Mech. Min. Sci. & Geomech. Abstr.*, 33(3), 245-254. 1996.
- Youngs, DL. Time-Dependent Multimaterial Flow with Large Fluid Distortion, *Numerical Methods for Fluid Dynamics*, 1982.